ECRONICON OPEN ACCESS

EC GASTROENTEROLOGY AND DIGESTIVE SYSTEM

Research Article

Method of Infrared Thermography for Earlier Diagnostics of Gastric Colorectal and Cervical Cancer

Yaniv Cohen[1]*, Ben Zion Dekel[2], Evgenii Krouk[1] and Nathan Blaunstein[3]

[1]School of Electronic Engineering Institute of Electronics and Mathematics (MIEM HSE), National Research University Higher School of Economics, Moscow, Russia

[2]School of Electrical and Computer Engineering, Ruppin Academic Center, Emek Hefer, Israel

[3]School of Electrical and Computer Engineering, Ben Gurion University of the Negev, Beer-Sheva, Israel

***Corresponding Author:** Yaniv Cohen, School of Electronic Engineering Institute of Electronics and Mathematics (MIEM HSE), National Research University Higher School of Economics, Moscow, Russia.

Received: August 26, 2019; **Published:** September 16, 2019

Abstract

This work describes an *in-vivo* non-contact and non-invasive skin temperature of mice with a detection of miniscule temperature changes, by using infrared thermo-cameras and comparing these changes with the surrounding area and with non-infected control skin areas. It was found that highly significant reduction in temperature can be produced by relatively small tumors. As a result metastasis less than 1 mm detection were observed. The explanation of this effect is related with the poorly vascularized nature of rapidly growing tumors. It was shown that by using heating or cooling technique, is possible to detect early tumors that starts in the subcutaneous propagating to the outer skin by using application of ethanol in order to emphasize small changes in temperature that starts deeper in the skin and it is difficult to detect them by visual optics. In addition, it was shown that after removing the tumor, skin temperature measured was the same as normal skin temperature.

We have found also that tumors in the size of 3 - 4 mm are 2.0°C colder than the surrounding area and small metastasis less than 1 mm are 0.5°C colder than the surrounding area.

The described results in this work, shows the ability of cancerous tumor early detection and the option to monitor tumor removal healing process by using a sensitive thermal camera following heating or cooling technique.

Keywords: *Colon; Gastro; Cancer; Thermal Imaging; Mice; Cooling and Heating*

Abbreviation

IR: Infra Red

Introduction

During the recent decades it was stated by the scientific society a few common intrinsic cancers associated with orifices and the current art methods of diagnosis. Various technologies, techniques and methodologies, and the corresponding embodiments were proved and configured for detection, imaging (e.g. visualization) and identification of the stomach, gastric colorectal and cervical cancers, lung cancer, cancer of the esophagus, and breast cancer, as well as different types of internal tumors, lesions, and other inner cancers by

combined visible and infrared (IR) optical signals based on integral regime (for visualization) and spectral regime (for identification) leading to earlier diagnosis and treatment of potentially dangerous conditions [4,11-17].

Stomach cancer: Stomach cancer (cardia and non-cardia gastric cancer combined) remains an important cancer worldwide and is responsible for over 1,000,000 new cases in 2018 and an estimated 783,000 deaths (equating to 1 in every 12 deaths globally), making it the fifth most frequently diagnosed cancer and the third leading cause of cancer death [1].

Colorectal cancer: Over 1.8 million new colorectal cancer cases and 881,000 deaths are estimated to occur in 2018, accounting for about 1 in 10 cancer cases and deaths. Overall, colorectal cancer ranks third in terms of incidence but second in terms of mortality [1].

Gastric and colorectal cancers are among the most common cancers in the world and therefore a lot of attention of not only medical society was accumulated on their earlier non-invasive diagnosis by use of various physical and engineering approaches based on different optical, acoustical, magnetic and X-ray devices. Namely, in visual optics the main goal is to use standard methods and the corresponding apparatus for screening gastric and colorectal cancers based on endoscopy tests by visual camera and biopsy sampling.

The human body sometimes develops tumors and other internal legions which destroy the functionality of affected organs and ultimately lead to death. Their early identification is critical for the health and survival of the patients.

Human body radiates naturally in the IR (infrared) range [6] and each tissue either normal or not normal, has its heat signature [2,3]. In this work, the proposed IR approach is based on passive imaging of heat signature changes in tumors due to minute changes of environmental temperatures around these tumors that may allow for screening and for characterizing these tumors more accurately at the earlier stages of their spatial-temporal evolution.

As today, IR cameras and Focal Plan Arrays (FPA) are getting smaller (See figure 1 from [7]), for example, Atto640 640 x 480 microbolometer detectors with a pixel pitch of 12 μm from LYNRED [22], or the M80 80X80 microbolometer from LYNRED [8,23], or FLIR-ONE IR thermal camera used with smart phones [24]. It can be used has a new tool for *in-vivo* endoscopy imaging to improve detection together with visual imaging.

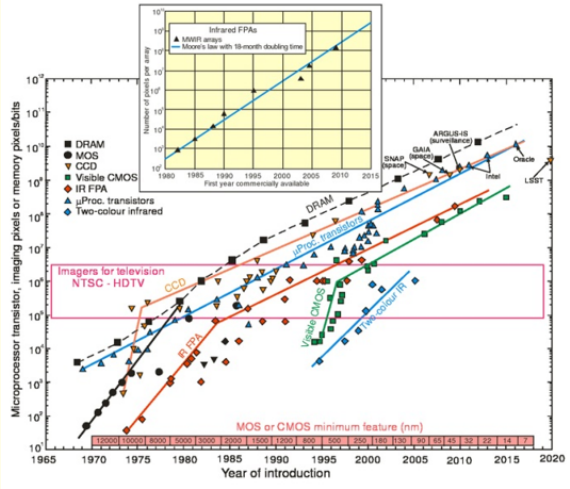

Figure 1: *Imaging array formats compared with the complexity of silicon microprocessor technology and dynamic access memory (DRAM) as indicated by transistor count and memory bit capacity. The timeline design rule of MOS/CMOS features is shown at the bottom [7].*

In this work, we will show the ability to detect small tumors and metastasis on mice that are not visible by naked eye or by visual camera, using a thermal camera with heating or cooling technique that can also be used for tumor removal monitoring. Also, *in-vitro* thermal imaging of Laparoscopic procedure for removing tumors filmed to show the thermal difference between normal tissue and tumors.

Current state of the art

Identification of Polyps [20] - Clinical Needs

Approaches to improve adenoma detection have either targeted endoscopic blind spots (behind folds, flexures) or visualized subtle lesions in the field of view (e.g. flat and depressed lesions). Much of the efforts to date have been on improvements to the endoscope (high-definition, narrow-band imaging, autofluorescence, and so forth) or contrast agents (molecular imaging, chromoendoscopy), which have been reviewed recently [21].

Flat dysplasia detection [20] - Clinical need

Flat dysplasia is the hallmark for carcinogenesis in Barrett's and ulcerative colitis. The current state of the art is multiple random biopsy specimens looking for the proverbial needle in the haystack. However, obtaining a large number of random biopsy specimens is tedious, expensive, adds potential complications, and results in potential false negatives (because typically < 5% of mucosa is sampled).

Theoretical background of the IR tomography and IR spectroscopy of cancerous and anomalous biological structures detection and identification

During recent years it was developed a novel infrared (IR) technology and the corresponding theoretical framework and techniques in conjunction with low-loss, flexible optical fibers, sensors and probes. This combination of visual and IR sensors with the corresponding spectrometers was adapted for different fields of application, including:

a) Non-invasive medical diagnostics of different kinds of external and internal superficial cancers, such as skin, cervical, gastric, and other different diseases, *in-vivo*.

b) Minimally invasive diagnostics of tissue.

c) Imaging and identification of organic (polymers) and biological structures and materials.

d) Remote monitoring of tissue, chemical processes and environmental features.

e) Characterization of the quality of foods as fruits and vegetables.

The developed of non-invasive, fast, compact, remote, portable and highly sensitive diagnostic methodology and the corresponding tool, based on measurements of the contrast of the temperature difference against the background and environment and its dependence on the wavelength in full spectra from 200 nm to 900 nm (visual optics) and from 1,000 nm to 20,000 nm (IR optics), were very promising for on-surface and sub-surface (up to few mm) analysis at the microcell level without any sample preparation.

Such nondestructive, non-invasive (or minimally invasive), fast (a spectra can be recorded in the time range of approximately a few seconds, up to ten seconds) and remote (the maximum fiber length can reach up to 2 - 3 meters) was proposed to be used for earlier diagnostics of internal cancers, such as gastric, colon, cervical, and stomach.

Based on modification of the canonical devices, such as endoscope, gastroscope, colonoscope, by introducing special IR sensors operating in the MIR bandwidth (that is 3 μm to 12 μm).

There are two methods for investigation of anomalous biological structures of different surfaces of human skin (outer and inner) by use IR tomography and IR spectrographic analysis, that is, the integral and the spectral regimes.

The IR-tomography is based on the integral method of the heat flows measurements from the analyzed structure's surface, and has the following technical difficulties and limitations, which we investigated and resolved it.

The integral method doesn't provide the classification of the substances, which the cancerous structures consist of, i.e. it is possible to detect the cancerous structures producing the heat flow anomaly, but it is impossible to accurately identify these structures. High accuracy can be obtained with spectral analysis, which was performed during our investigations of biological structures and organic materials, using IR bandwidth and skin cancer using visual optic bandwidth.

The detecting of the integral heat flows and their space distribution along the surface of the investigated structure, as well as further evaluation of these data to the values of temperature of the superficial structures are made without taking into account the difference between radiant patterns of all structure components. That is why, structure components, having different radiant patterns and different temperature values, will produce the same values of integral heat flow over the wavelength range under investigations.

In our analysis we dealt with the range of 200 nm to 800 nm (optical bandwidth) and with 800 nanometer to 40 micrometer (IR bandwidth). For this reason, it is clear why some cancerous structures or biological objects were detected. In contrast to, the homogeneous surfaces with the same temperature gradients, which can provide a wrong signal, that is, the noise instead of real information on the biological structure. To overcome this limitation we used IR-spectrograph for spectral analysis.

The mentioned limitations are solved using of both integral and spectral methods of biological structures detection and identification presented by the proposed framework that allows us to use it for operative practice of earlier stages of superficial cancers diagnostics, such as skin, stomach, gastric, cervical and colon cancers. Therefore, the main goal of the proposed framework is to provide a device for reliable detecting, revealing the exact location, and classification of the substances forming the revealed cancerous structures.

The biological zones radiate heat flow from the human body, caused by any anomalous structure, can be detected by IR detector. In this regime the anomalous heat radiation from surface are characterized by the so called heat contrast C:

$$C = \{J'(\lambda) - J''(\lambda)\} / [J'(\lambda) + J''(\lambda)], \quad (1)$$

where $J'(\lambda)$ - the heat flow from the regular surface structure at the human body which do not have any anomaly, $J''(\lambda)$ - the heat flow from the biological structure having anomaly (See figure 2).

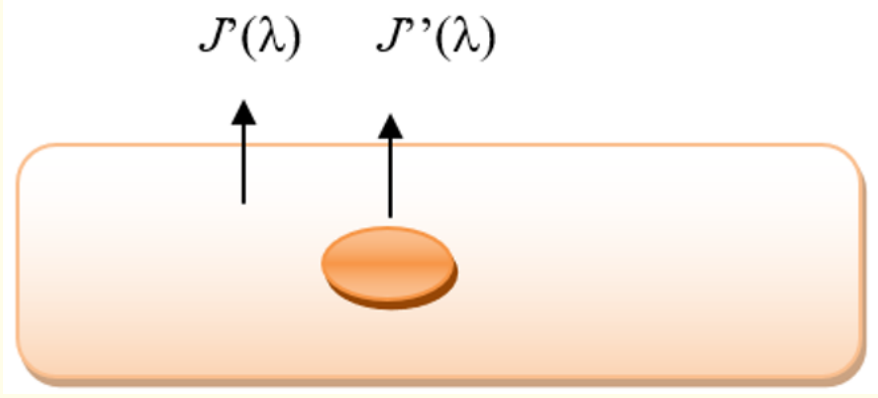

Figure 2

The absolute properties of these heat flows may be defined by the following expressions:

$$J''(d\lambda) = \int_{\lambda_{min}}^{\lambda_{max}} [dJ(\lambda,T)/d\lambda]\{\varepsilon_S(\lambda)\,\tau_a(\lambda) + \varepsilon_a(\lambda)\tau_s(\lambda)\}d\lambda, \quad (2)$$

$$J'(d\lambda) = \int_{\lambda_{min}}^{\lambda_{max}} [dJ(\lambda,T)/d\lambda]\,[\varepsilon_S(\lambda)\,\tau_a(\lambda)]d\lambda, \quad (3)$$

$$dJ(\lambda,T)/\delta\lambda = C_1\lambda^{-5}[\exp(C_2/\lambda T) - 1]^{-1}, \quad (4)$$

ε_s - The heat radiation coefficient (emissive coefficient) of the skin at T~310K.

τ_s - The transparent coefficient (transparency) of the human skin at T ~ 310K.

ε_a - The heat radiation coefficient (emissive coefficient) of the anomalous structure at the human skin at T ~ (310K + dT),

τ_a - The transparent coefficient (transparency) of the anomalous structure at the human skin at T ~ (310K + dT), parameters C_1 and C_2 are defined from results of measurements and equal: C_1 = 3.74 10-16 W/m^2; C_2 =1.44 10^(-2) mK;

dT is the deviation of the regular temperature due to anomaly existing at the human tissue's surface, that is defined by metabolic characteristics of the heating process described by a well-known equation of thermodynamics.

It was obtained empirically via numerous measurements with thermo coupling device *in-vivo* in real time (See Table 3.1, according to [3,4]).

As follows from Table 3.1, abnormal tissue temperature is slightly higher than normal tissue, temperature differences between normal and malignant tissues, Statistical analysis showed that ΔT greater than 1.7°C, constitutes a crucial point for the diagnosis of malignancy, in stomach lesions, with sensitivity (72%) and specificity (94%).

Type of lesion	Cases	Temperature differences (ΔT) (°C)	Angiogenesis (micro-vessels count)
Hyperplastic	8	0.75 ± 0.39	44.2 ± 37.4
Gastritis	19	1.19 ± 0.21	78.2 ± 24.4
Ulcer	9	1.44 ± 0.29	82.8 ± 28.5
Dysplasia	7	1.60 ± 0.48	83.0 ± 18.6
Adenocarcinoma	11	2.20 ± 0.55	83.1 ± 51.0

Table 1: *Temperature differences and levels of angiogenesis (mean, SD) by type of lesion.*

Spectral regime

The spectral density of radiated thermal flow is the function of the gradient-gradient of temperature and the narrow bandwidth $\Delta\lambda_i$, that is, the counting of the mean spectral density of the measured heat flows in each band of measuring according the formula:

$$S\lambda i = J\lambda i / \Delta\lambda i, \quad (5)$$

where $S\lambda_i$ is the mean spectral density of the heat flow for the chosen

λ_i band (i^{th} wavelength),

$J\lambda_i$ - the measured value of the heat flow in the chosen λ_i - band,

$\Delta\lambda i$ - spectral width of the chosen i^{th} band.

The desired goal is achieved by the following operations:

a). The measuring of the space distribution of the integral heat flow radiated from the biological structure in the range of wavelength from 1 - 2 μm up to 40 μm and more.

b). The detecting and outlining of the anomalies of the heat flow radiated from the structure's surface, and the following additional operations:

c). The classification of the causing the detected anomalies of biological structure by the sign and the absolute value of the heat flow changes, that is, by the sign and amplitude of the contrast of the desired biological structure.

d). The heat flow measuring in the anomalous zones in the chosen wavelengths with the narrow wave band measurements.

e). The final classification of the foreign anomalies by using the totality of the data measurements.

The distinctive feature of the proposed method from the future engineered device is that additional operations are introduced [operations from items (a) to (e) and formulas (1)-(5)]. Indeed, as follows from formulas (2)-(5), the anomalous radiated flow is proportional to the gradient of temperature, and then, from formula (1) follows that the contrast is proportional to the "gradient-gradient temperature", or to its second derivative, that is,

$$C \sim \Delta J(\lambda) = \Delta(T), \text{ where } \Delta(T) = \nabla(\nabla T) \qquad (6).$$

And what is important to outline is that this second derivative, or contrast, is a function of wavelength λi taken during real-time measurements by the proposed device. The proposed technology, when the sensitivity and SNR allow us, to identify more precisely changes in temperature, which are very small (of about 0.1 - 0.5 Kelvin) observed in anomalous structures of human tissues.

Cooling and heating of cancerous structures

As was reported in [2], for intrinsic cancer and then observed experimentally for oral cancer [5], thermal "response" of cancerous structure differs from that of the regular tissues. As will be shown below experimentally in Section 3 "reaction" on heating and cooling of cancerous tissues also differs comparing to that of normal tissues. As follows from equations (1)-(4), metabolic processes of any anomaly cell of tissue occurs on the molecular level in different manner and reflect different thermo-diffusion processes with different parameters of thermo-conductivity or thermo-transparency (τs and τa) presented in the corresponding thermodynamic integral equations (2)-(3). This is important feature because, as will be seen from experiments carried out ourselves and reported in Section 3, sometimes it is impossible to detect tissue anomalous located deeper inside human skin by use integral regime of thermo-imaging. In this case was proposed the method of cooling and heating of the skin regions under test. Let us explain briefly what it means. In figure 3, we show two cells - anomaly with temperature T" (the color cell in figure) and regular background with temperature T' (the color "plate" in figure) which generate different heating flows with intensities J' and J", respectively. As it follows from equations (1)-(5), in all cases these intensities are functions of the irradiated.

Now, let us consider that we heat these two tissues, by a heating flow with intensity J"', as is shown in figure 4. Because there is difference between temperatures, T"' and T", T"' and T', we have, according to Equation (6) the following relations:

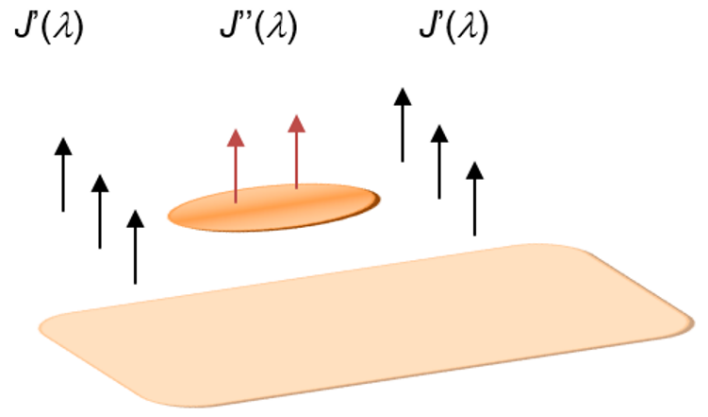

Figure 3

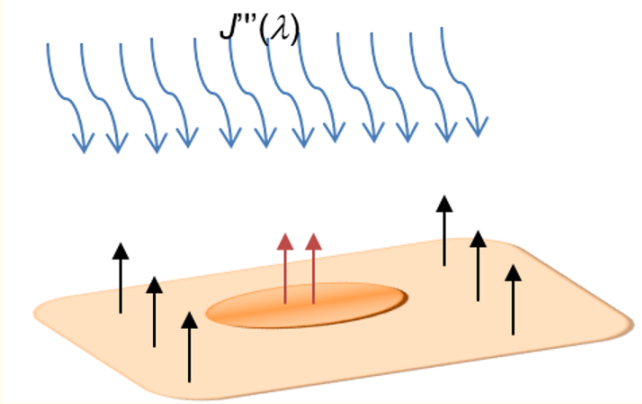

Figure 4

$\Delta J_1(\lambda) \sim (T'''-T') = dT_1$ - for regular tissue (7a)

$\Delta J_2(\lambda) \sim (T'''-T'') = dT_2$ - for cancerous (anomaly) structure (7.b)

Then, due to faster relaxation of temperature of the normal tissue with respect to the anomalous one, that is, dT1/dt > dT2/dt, it can be identify the anomalous structure "hidden" into the regular tissue environment. The same will be with cooling where the speed of relaxation of the normal tissue will be higher than that for the anomalous tissue. All these effects obtained experimentally, will be discussed below in Section 4. This method was taken from reference [17].

Diameter and depth of the tumor: The paper by Kosus., *et al*. [18] shows the diameter and depth of the tumor as a problem to be solved using thermal techniques, using the width at half height (FWHM) to estimate the depth of a small heat source of the isothermal distribution hot spots area.

Furthermore, because of the complex structure of breast heat transfer, the application of a vascular model requires detailed knowledge of the microvascular network. Therefore, the Penne's bioheat equation (8) was used to model the heat transfer in the breast:

$$pc\frac{\delta T}{\delta t} = \nabla \cdot k\nabla T - w_b p_b C_b (T - T_b) + O_m \quad (8)$$

Where p, c and k denote the density, specific heat, and thermal conductivity of the tissue. p_b and C_b are the density and specific heat of the blood; w_b (mL/s/mL) is the blood perfusion rate; O_m is the metabolic heat generation, T_b is the supposedly constant arterial blood supplier temperature, and T is the breast temperature. To determine the relationship between depth and heat transfer during cooling, it is useful to define the depth of thermal penetration; unfortunately, this is not yet accurate due to the complex structure of the breast. However, a hypothesis can be made considering the hemispheric domain. Moreover, it appears that after cooling of the breast, the response time (the heat detected on the surface of the breast) increases with the depth of the tumor. We also observed that the diameter of the tumor has no significant effect on the response time for shallow tumors, and that the smaller the tumor, the longer the response time. During our experiment, we observed some principles to measure correct values, and also to make our thermal sensor more accurate [19]. One of the essential procedures that we found to be important was to maintain the room temperature between 18 and 22°C, so that the total heat loss can be considered proportional to $(T_s - T_f)$, provided that $(T_s - T_f)$ is small. Thus, the boundary condition at the breast surface has been reduced as shown in Equation (9), with a surface conductance defined in equation (10).

$$-k\frac{\delta T}{\delta t}\Big|_{skin} = h_0 (T_s - T_f) \quad (9)$$

where h_0 is called a constant of surface conductance which is composed of radiative and convective components.

$$h_0 = h_{conv} + h_{rad} \quad (10)$$

A typical maximum transient thermal contrast during warming for a breast with a 10 mm tumor at a depth of 5 mm after being cooled for 1 minute was shown in this article. At the time of reading of the thermal graph processes by the computer, the amplitude of the transient peak and its corresponding time, as well as the response time, were extracted from the maximum transient thermal contrasts for tumors of different diameters located at different depths. This analysis shows the peak of the temperature generated on the surface of the breast with the tumor. As shown in the diagram in figure 5, the area surrounding the tumor will produce more heat during the warming phase before falling back to a stable temperature.

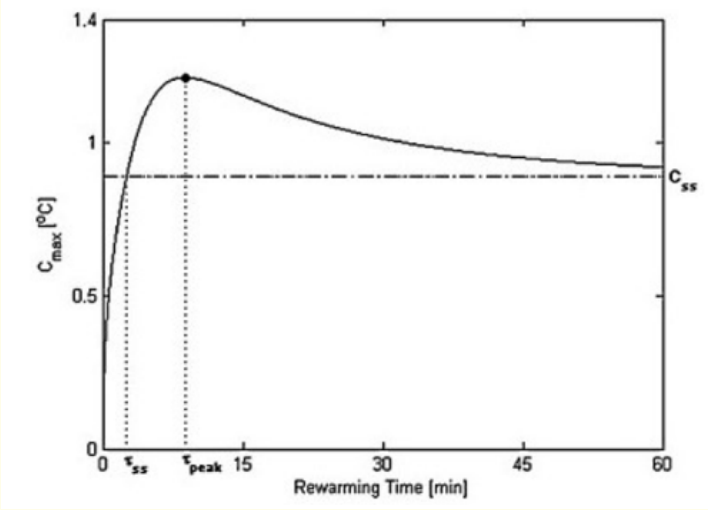

Figure 5

Experimental clinical tests

Digital infrared thermal imaging of tumors in mice

The study presented in the current work, was approved by the ethics committees of Hadassah medical center, Israel and was conducted in accordance with the Declaration of Helsinki, NIH approval number: OPRR-A01-5011.

Four groups, each containing 10 mice, injected subcutaneously as follow:

- Group 1: Injected with H460 (mouse lung tumor).
- Group 2: Injected with MMAC (mouse mammary adenocarcinoma).
- Group 3: Injected with both types but at different sites.
- Group 4: Injected with medium only- serve as control.

It should be noted that these tumors usually develop locally with no metastasis within the 20 day period in which we propose to screen the tumors.

One day after and subsequently for 18 additional days all groups will be anesthetized and screened for specific temperature changes. Also, at each point one mouse from each group will have its peritoneum exposed, scanned and it will be sacrificed. Biopsies of internal organs and skin will be harvested and sent for pathological examination in order to correlate tumor growth with the results obtained from the thermographs.

The digital infrared images were collected using thermal camera "Gilboa" by OPGAL LTD, (https://www.opgal.com/), Pixel Size - 25 μm, Spectral Range - 7.5-14 μm , Number of Pixels – 640 x 480, Thermal resolution - 70 mK, Focus - 12 cm, Lens - 18 mm, FOV - 25.5 degrees. In figure 6a-6c the setup of the animal clinical trial is shown.

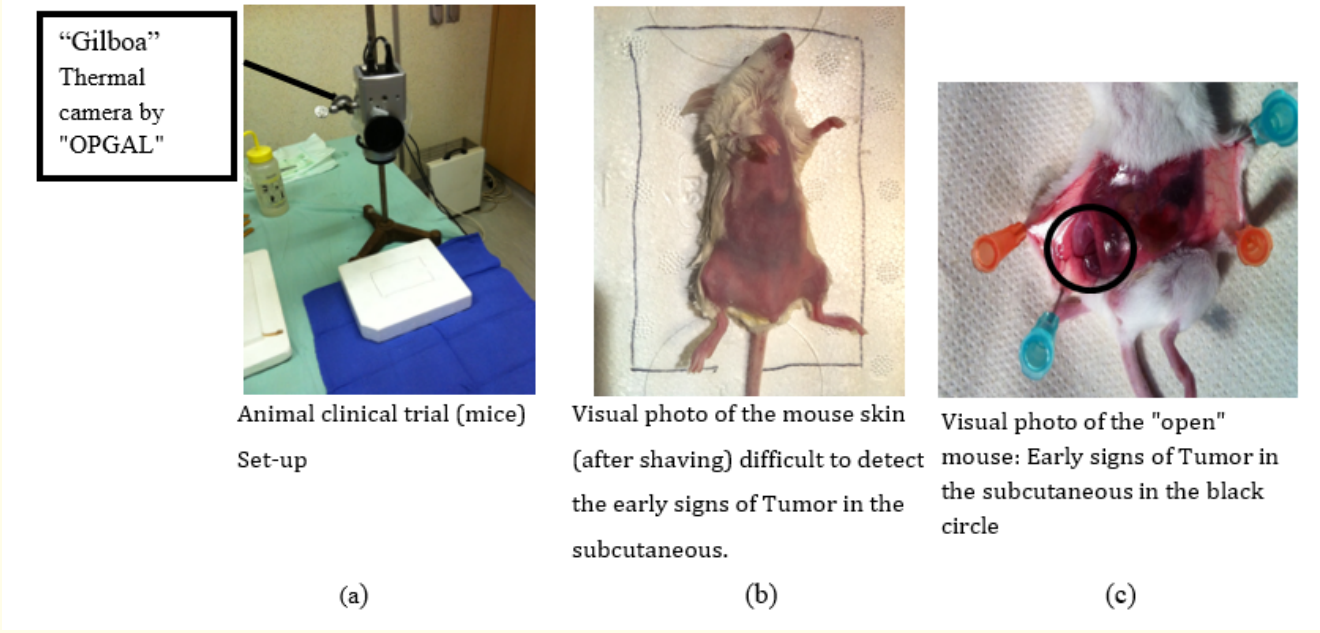

Figure 6

Figure 7 shows outer thermal photo of the mouse skin after shaving, after its visualization (See figure 6b). As clearly seen from the presented figure, it is difficult to detect the early signs on the skin of Tumor that starts in the subcutaneous.

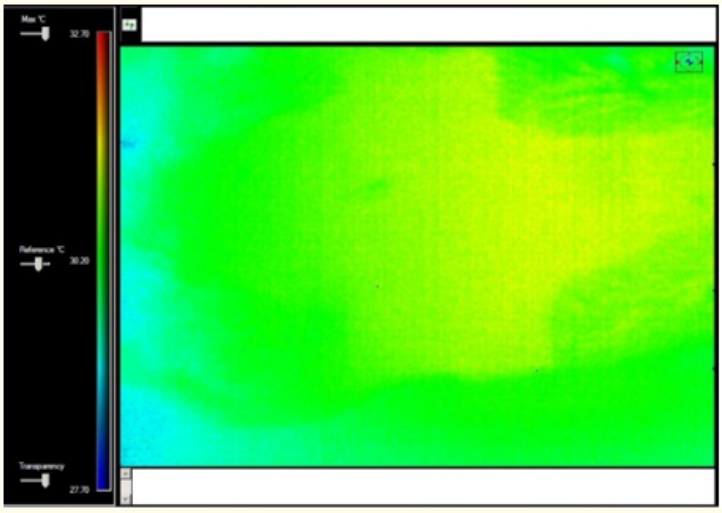

Figure 7

To analyze dynamic of small tumor metastasis creation, in the second part we opened the mouse bally and ravel the sub-cutaneous tumor, as it is visualized in figure 6c. The corresponding results are shown in figure 8a and 8b.

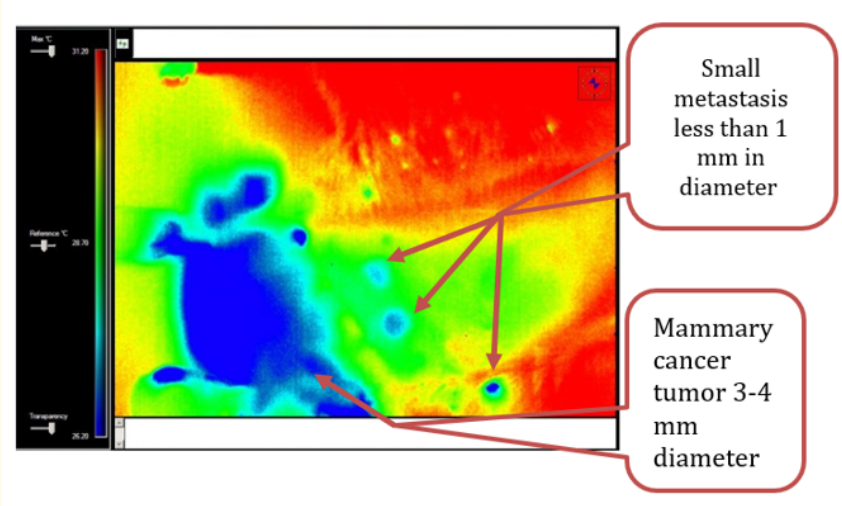

Figure 8a: *Animal Mammary Cancer Metastasis (blue colored dots showed by arrows); a close-up image of a mouse open bally metastasis: less than 1-mm diameter.*

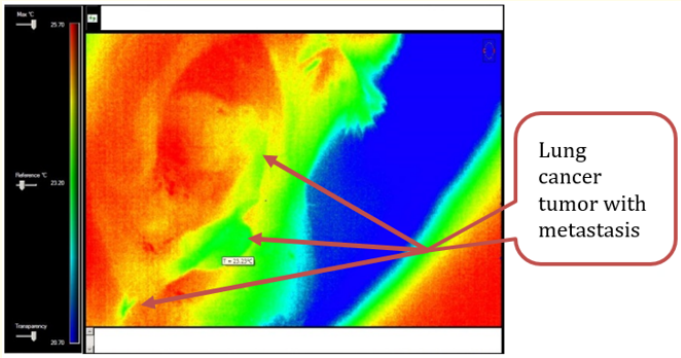

Figure 8b: *Lung Cancer with Metastasis (shows in arrows).*

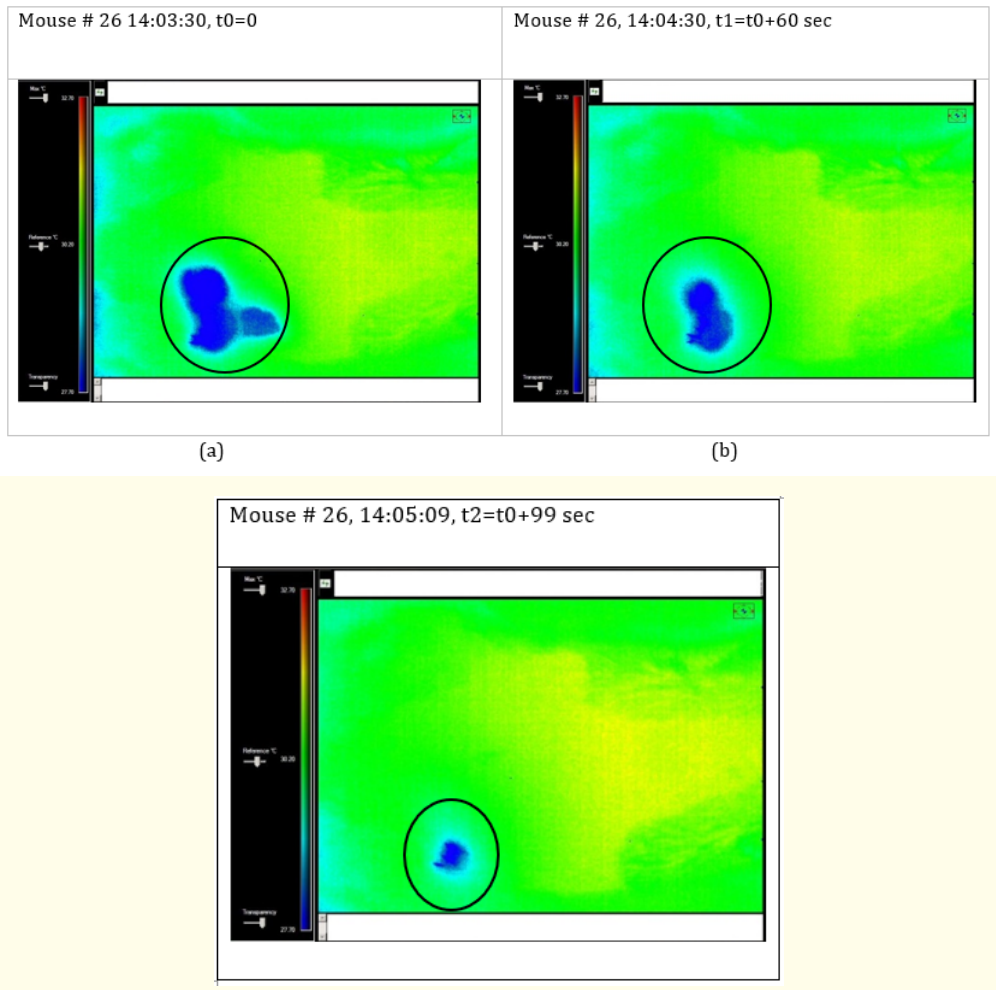

Figure 9

Cooling and heating

In the third part of clinical trials, after shaving of the mice skin, as shown in figure 6b, all bally outer skin was cooled by application of ethanol.

As it is shown in figure 9a-9c, due to different temperature gradient of tumor (shown by blue color) and normal skin (shown by green and yellow color) it was detected by thermal camera. Tumor area remain colder than normal skin with time.

Tumor removal monitoring

At the forth part of clinical trial, after opening of mouse bally, the tumor removal procedure was carried out and a set of thermal imaging photos were taken.

Figures 10a to 10d present results of this procedure. Thus, figure 10a presents a sub-cutaneous tumor by blue color that is, showing its colder behavior comparing with the surrounding tissue (green color).

Figure 10b describes the tumor removal procedure using Scissors and Tweezers. Again, a tumor is colder than the surrounding tissue.

Figure 10c presents the partially removal of tumor. As it is clearly seen, after removal of part of the tumor, the temperature of the cutting area, from which the tumor was removed, matches the normal skin temperature changed from blue to green color.

Figure 10d shows the full tumor removal. It is seen that after removal of the tumor, the tissue temperature matches the normal skin temperature (changed from blue to green color). The blue contour surrounding the removal area of the removal tumor is the Metastasis of the tumor that cannot be visualized by visual optics. Indeed, the thermal camera can show difference between the removal area, normal skin and peculiarities of the tumor including metastasis.

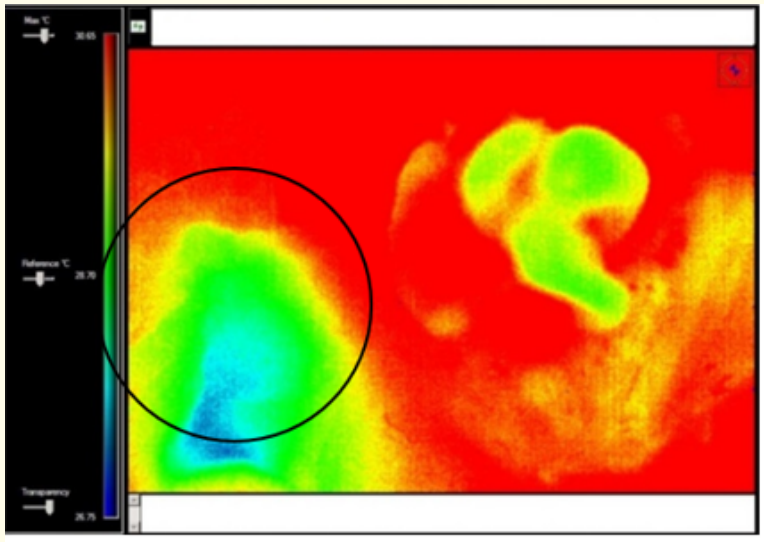

Figure 10a: *Mouse#36, Thermal photo of the mouse open bally, before removal of the tumor (blue colored and circle).*

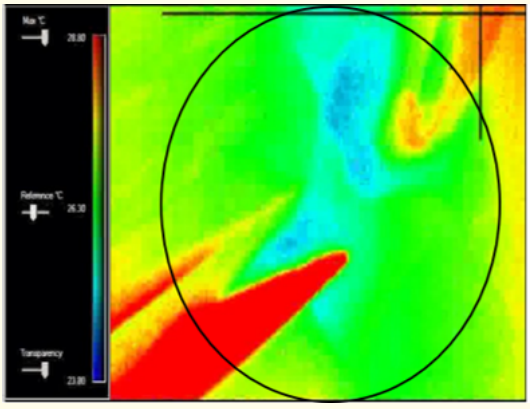

Figure 10b: *Mouse # 36, Thermal photo of the mouse open bally, during removal of the tumor using scissors and tweezers.*

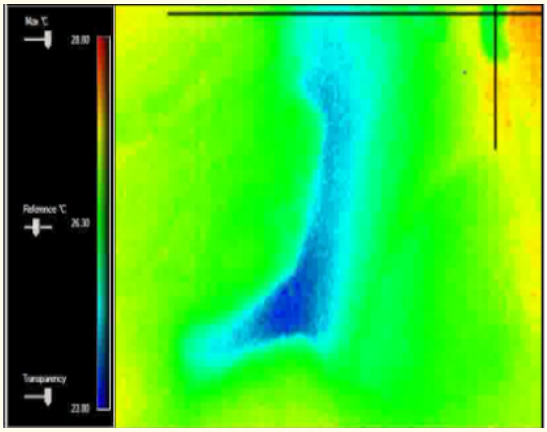

Figure 10c: *Mouse # 36, Thermal photo of the mouse open bally, during removal of the tumor, not removed completely.*

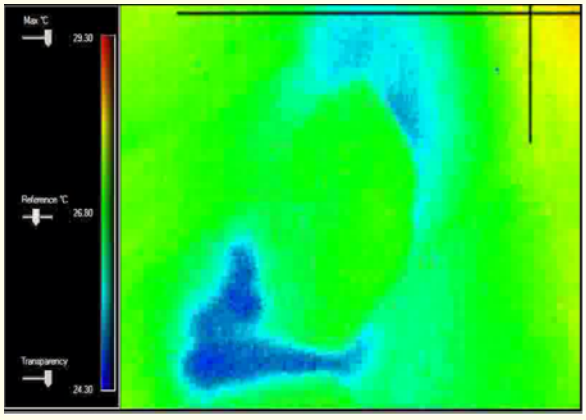

Figure 10d: *Mouse # 36, Thermal photo of the mouse open bally, during removal of the tumor, not removed completely.*

In-vitro thermal imaging by use of Laparoscopic procedure

During the recent study, a preliminary test was performed *in vitro*. The OPGAL IR camera was used to film a Laparoscopic procedure for removing tumors from the large intestine. Figure 11a shows the using set-up. Figure 11b presents thermal picture of the procedure.

(b) "OPGAL" IR thermal camera

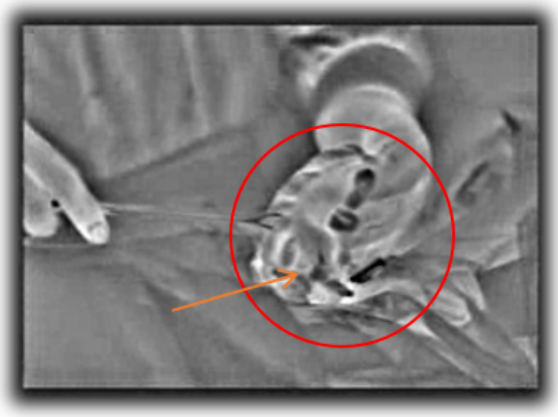

(a) Black and white thermal picture of a tumor (black=colder; white=warmer)

Figure 11

Then, the same procedure was carried out by use the pseudo-colored thermal picture of a tumor (Blue, Green=cold; white=warm, Red - warmer), Figure 12 presents *in-vitro* thermal picture (left panel) and visual picture (right panel) of a tumor outside of the colon 1-minute after disconnecting tumor from blood supply.

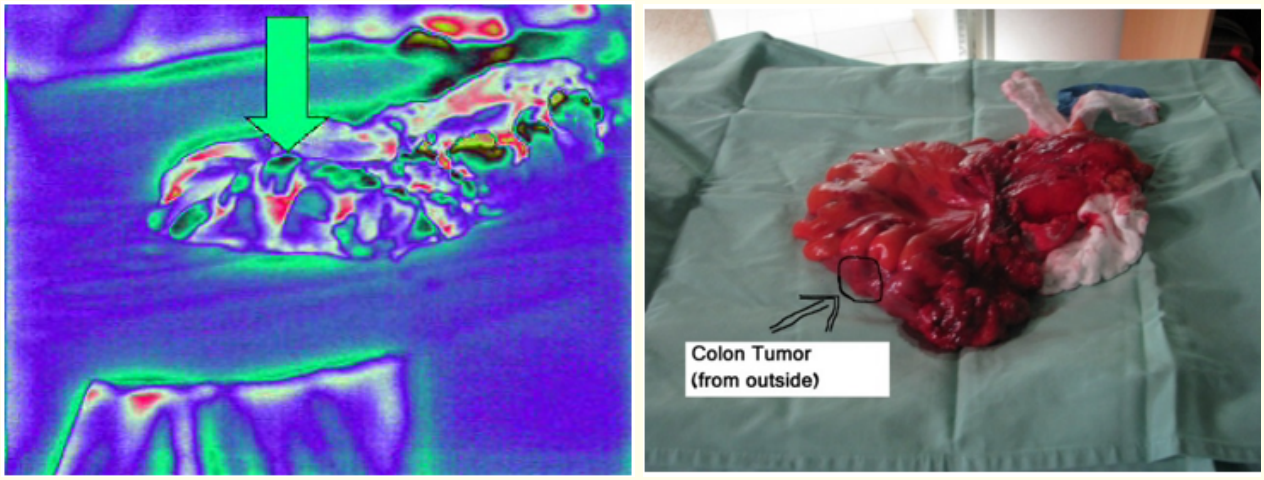

Figure 12

The same *in-vitro* thermal picture outside of the colon 2-min after disconnecting tumor from blood supply is shown by figure 13.

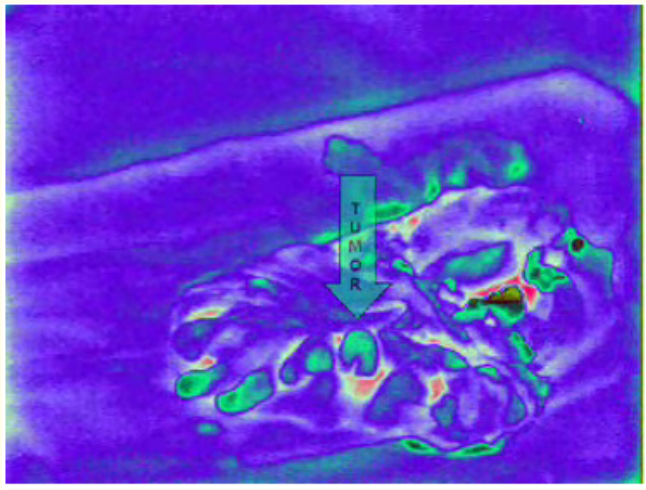

Figure 13

At the later stage of the procedure, thermal picture inside the colon 7-minutes and 10-minutes after disconnecting tumor from blood supply is shown in figure 14a and 14b, respectively.

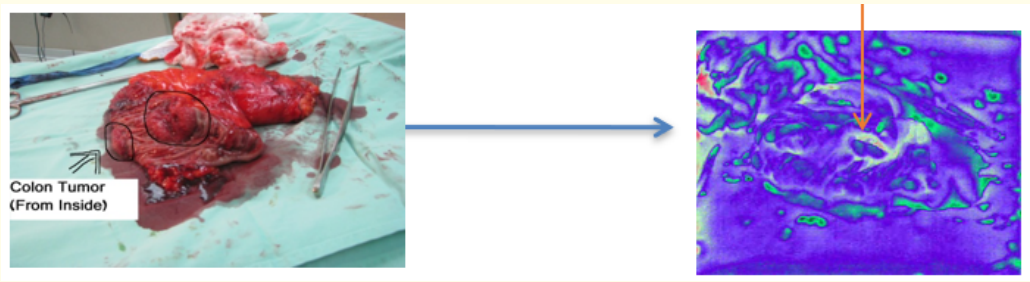

Figure 14a: *7-minutes after disconnecting the tumor.*

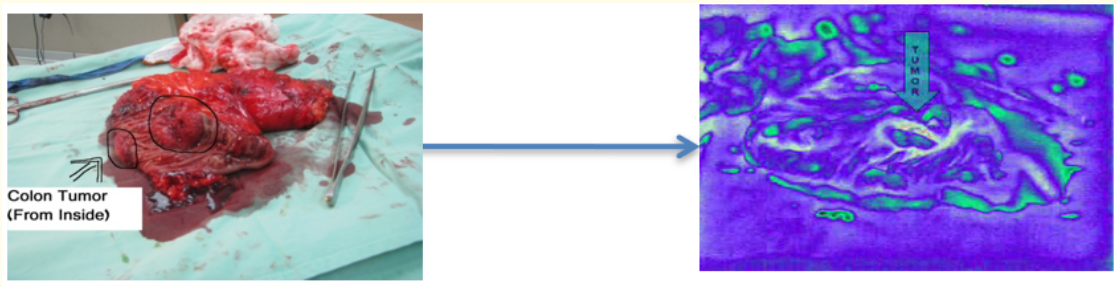

Figure 14b: *10-minutes after disconnecting the tumor.*

As can be seen from above clinical trials, the tumor is hot compared to normal tissue (seeing in the red and white colors). Moreover, using thermal camera, we able to differentiate thermal features of the tumor with respect to surrounded normal tissue. After cooling of the colon with the tumor inside, the temperature difference of the tumor remains the same compared to cooling of normal tissue.

Results and Discussion

By using a non-contact and non-invasive infrared thermo-cameras we were able to monitor and detect surface skin mice miniscule temperature changes. The *in vivo* measurement compares these changes with the surrounding area and with non-infected control skin areas. It was found that highly significant reduction in temperature differences can be produced by relatively small tumors. As a result, small metastasis less than 1 mm detection were observed. The explanation of this effect is related with the poorly vascularized nature of rapidly growing tumors [9,10].

Tumors in the size of 3 - 4 mm are 2.0°C colder than the surrounding area. Small metastasis less than 1 mm are 0.5°C colder than the surrounding area.

By using the heating or cooling technique we were able to early detect tumor that starts in the subcutaneous propagating to the outer skin by using application of ethanol to emphasize the small changes in temperature that starts deeper in the skin and hard to detect by visual optics.

After removal of tumor, the measured skin temperature was the same as the normal skin temperature. In case the tumor was not remove completely, a temperature difference was shown.

Conclusion

In summary, we have shown the ability for an early detection of tumors and the ability to monitor tumor removal by using a sensitive thermal camera and by heating or cooling technique.

The present findings are important as they show that cancer removal can be monitor non-invasively to ensure complete removal and early detection of cancer inside/outside of the human body.

Using thermal imaging technique following cooling or heating the skin surface, may have an important role for the development of next-generation techniques for *in vivo* tests for the detection of tumors which cannot be detected by human or conventional machine vision systems

Our following research includes developing a bio-physical model which will predict the status of the suspected tissue. The model is based on the camera intensities recorded as function of time of the digital image as the independent variables, and the tumor size, temperature and type as the depended variables.

Bibliography

1. Bray F., *et al*. "Global cancer statistics 2018: GLOBOCAN estimates of incidence and mortality worldwide for 36 cancers in 185 countries". *CA: Cancer Journal for Clinicians* 68.6 (2018): 394-424.

2. B Dekel., *et al*. "Method of Infrared Thermography for Earlier Diagnostics of Gastric Colorectal and Cervical Cancer". In: Chen YW, Tanaka S, Howlett R, Jain L. (Editors) Innovation in Medicine and Healthcare 2016. InMed 2016. Smart Innovation, Systems and Technologies, vol 60. Springer, Cham (2016): 83-92.

3. S Christodolos and C Christina. "Thermal Heterogeneity Constitutes A Marker for the Detection of Malignant Gastric Lesions In Vivo". *Journal of Clinical Gastroenterology* 36.3 (2003): 215-218.

4. G Theophilou., *et al*. "ATR-FTIR spectroscopy coupled with chemometric analysis discriminates normal, borderline and malignant ovarian tissue: classifying subtypes of human cancer". *Analyst* 141.2 (2016): 585-594.

5. BZ Dekel., *et al*. "Diagnosis of oral cancer based on FTIR-ATR spectra of salivary exosomes-Preliminary study". Proceedings of NBC Conference (2017): 3.

6. N Shussman and Y Mintz. "Laparoscopic Infrared Imaging-The Future Vascular Map". *Journal of Laparoendoscopic and Advanced Surgical Techniques* 21.9 (2011): 797-801.

7. A Rogalski. "Next decade in infrared detectors". Proceeding SPIE 10433, Electro-Optical and Infrared Systems: Technology and Applications XIV, 104330L (2017).

8. P Robert., *et al*. "Low power consumption infrared thermal sensor array forsmart detection and thermal imaging applications". AMA Conferences 2013-SENSOR 2013, OPTO 2013, IRS 2 (2013).

9. Xie W., *et al*. "Evaluation of the ability of digital infrared imaging to detect vascular changes in experimental animal tumours". *International Journal of Cancer* 108.5 (2004): 790-794.

10. Song C., *et al*. "Thermographic assessment of tumor growth in mouse xenografts". *International Journal of Cancer* 121.5 (2007): 1055-1058.

11. Berz Reinhold and Claus EE Schulte-Uebbing. "MammoVision (Active Functional Infrared Breast Thermography) Compared to X-Ray Mammography-114 Cases Evaluated" (2010).

12. BB Lahiri., *et al*. "Medical applications of infrared thermography: A review". *Infrared Physics and Technology* 55.4 (2012): 221-235.

13. Ćurković S., *et al*. "Medical thermography (digital infrared thermal imaging-DITI) in paediatric forearm fractures-A pilot study". *Injury* 46.6 (2015): S36-S39.

14. Sivanandam S., *et al*. "Medical thermography: a diagnostic approach for type 2 diabetes based on non-contact infrared thermal imaging". *Endocrine* 42.2 (2012): 343.

15. Magalhaes C., *et al*. "Recent use of medical infrared thermography in skin neoplasms". *Skin Research and Technology* 24.4 (2018): 587-591.

16. Saira Chaudhry., *et al*. "The use of medical infrared thermography in the detection of tendinopathy: a systematic review". *Physical Therapy Reviews* 21.2 (2016): 75-82.

17. Sebastien Jean Mambou., *et al*. "Breast Cancer Detection Using Infrared Thermal Imaging and a Deep Learning Model". *Sensors (Basel)* 18.9 (2018): 2799.

18. Kosus N., *et al*. "Comparison of standard mammography with Digital mammography and Digital infrared thermal imaging for breast cancer screening". *Journal of the Turkish-German Gynecological Association* 11.3 (2010): 152-157.

19. Mambou S., *et al*. "Breast Cancer Detection Using Modern Visual IT Techniques". In Modern Approaches for Intelligent Information and Database Systems; Andrzej S, Adrianna K, Manuel N, Quang Thuy H, Eds.; Springer: Berlin, Germany, Volume 769 (2018): 397-407.

20. Roy Hemant K., *et al*. "Spectroscopic Applications in Gastrointestinal Endoscopy". *Clinical Gastroenterology and Hepatology* 10.12 (2012): 1335-1341.

21. Murthy S., *et al*. "Novel colonoscopic imaging". *Clinical Gastroenterology and Hepatology* 10.9 (2012): 984-987.

22. https://www.lynred.com/produit/atto640

23. https://www.lynred.com/produit/m80

24. https://www.flir.com/flirone

Volume 6 Issue 10 October 2019